QUARTERLY OF APPLIED MATHEMATICS
VOLUME XLIII, NUMBER 2
JULY 1985, PAGES 201–210

THE DYNAMIC 2D ANALYSIS OF A CONCENTRATED FORCE NEAR A SEMI-INFINITE CRACK*

BY

L. M. BROCK

University of Kentucky

Abstract. An exact dynamic 2D solution for a concentrated force near a stationary semi-infinite crack in an unbounded plane can be used in the transient analysis of wave-scattering problems. Direct approaches to obtaining the solution, however, are complicated by the existence of a characteristic length. A less direct approach is used here which circumvents these complications. As an example, the dynamic stress intensity factors are derived and studied for their behavior w.r.t. time and concentrated force-crack edge orientation.

1. Introduction. Wave-scattering studies of cracks, voids, dislocations and inclusions [1, 2] often require a knowledge of transient solutions to idealized wave propagation problems. For both analytical [3] and computational [4] convenience, these solutions are often based on the Green's function-related problem of a concentrated force. By adopting an eigenstrain [5] approach, in fact, the effects of a void or inclusion can be incorporated in the problem solution, although this has generally been done for ellipsoidal shapes, and in the frequency domain. Similarly, dislocations can be incorporated by treating them as body force terms [6] in the governing equations for the problem.

The mixed boundary conditions which arise make such an incorporation more difficult to realize for cracks. However, the advantages are perhaps even greater: the crack edge singular behavior and traction-free crack surface conditions are automatically built into a complete wave propagation problem based on superposition of the concentrated force solution.

This article, therefore, considers an exact 2D dynamic analysis of a concentrated force near a semi-infinite stationary crack in an unbounded, isotropic, linearly elastic plane. Crack problems can be treated [7] as the superposition of two problems: Problem 1 considers the disturbance in a crack-free geometry, here the concentrated force in the unbounded plane. Problem 2 considers only the crack, but with surfaces subjected to the

* Received March 12, 1984.

©1985 Brown University

negatives of the Problem 1 tractions induced over the region corresponding to the crack. This superposition approach is adopted here, but with some care; the crack edge-concentrated force separation give Problem 2 a characteristic length, thus complicating a standard solution approach.

The concentrated force problem is formally stated in Sec. 2. Subsequently, Problem 1 is stated and the solution given. Problem 2 is then addressed as a series of simpler problems. As an example of the resulting solution behavior, the crack edge stress field is then studied.

2. Concentrated force problem. Consider the crack defined in the xy-plane as $y = 0$, $x > 0$. The plane is at rest for $s < 0$, where s is the time multiplied by the dilatational wave speed. As $s = 0$ a unit concentrated force is applied as shown in Fig. 1a, where $d > 0, |\phi, \psi| \leqslant \pi$. The governing equations in the plane are then

$$\mathbf{u} \equiv \mathbf{0}\ (s \leqslant 0), \tag{2.1}$$

$$\nabla^2\mathbf{u} + (m^2 - 1)\nabla\Delta + \frac{1}{\mu}\mathbf{B} = m^2\ddot{\mathbf{u}} \qquad (s > 0) \tag{2.2}$$

where $\mathbf{u}(x, y)$ is the displacement vector with x and y-components (u_x, u_y), Δ is the dilatation, ∇ is the gradient operator, $(\cdot)$ denotes s-differentiation, μ is the shear modulus, ∇^2 is the Laplacian and $1/m$ is the non-dimensionalized rotational wave speed. Here all speeds are non-dimensionalized by division with the dilatational wave speed, so that $m > 1$. The body force in (2.2) is

$$\mathbf{B} = (\cos\phi, \sin\phi)\delta(x + d\cos\psi)\delta(y + d\sin\psi)H(s) \tag{2.3}$$

where $\delta(\ )$ and $H(\ )$ are the Dirac and Heaviside functions. The dimension of the unit concentrated force is that of force/length. Along both crack surfaces the traction $\mathbf{T}$ vanishes, i.e.

$$\mathbf{T}^{\pm} = \mathbf{0} \tag{2.4}$$

along $y = \pm 0$, $x > 0$, where its components are given by

$$\frac{1}{\mu}T_y = m^2\frac{\partial u_x}{\partial y} + (m^2 - 2)\frac{\partial u_y}{\partial x}, \qquad \frac{1}{\mu}T_x = \frac{\partial u_y}{\partial x} + \frac{\partial u_x}{\partial y}, \tag{2.5}$$

In addition, appropriate radiation conditions as $s \to \infty$ are required [8]. It should be noted that, in the sense of a Green's function, this problem is often [3, 8] defined by replacing the Heaviside function in (3) with $\delta(s - \xi)$, $\xi > 0$. Clearly, the solution for that definition will follow from the present solution by s-differentiation and then replacing s with $s - \xi$.

3. Problem 1. The governing equations for Problem 1 are identical to those presented above, except that (2.4) is deleted. That is, Problem 1 is essentially a 2D dynamic free space Green's function problem [3]. The solution written as a function of s and the

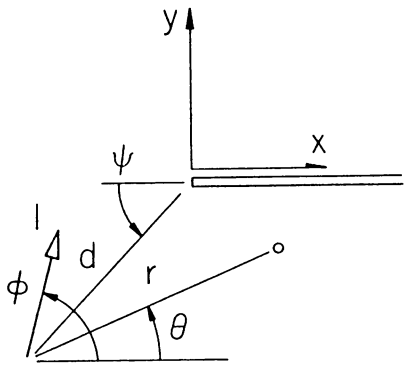

FIG. 1a. Point force-crack edge geometry.

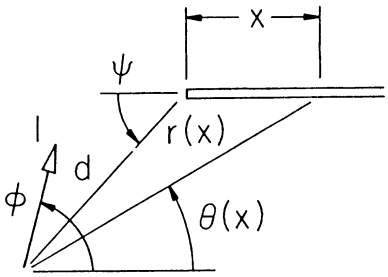

FIG. 1b. Polar coordinates (r, θ) along crack surface.

coordinates (r, θ) shown in Fig. 1a can be obtained from general results for an arbitrary **B** [9]. In particular

$$2T_x^* = 2H_{12}\sin(\phi - 3\theta) - H_1 \sin 2\theta \cos(\phi - \theta) - H_2 \cos 2\theta \sin(\phi - \theta), \quad (3.1)$$

$$2T_y^* = 2H_{12}\cos(\phi - 3\theta) - H_1(m^2 - \cos^2\theta)\cos(\phi - \theta) - H_2 \sin 2\theta \sin(\phi - \theta), \quad (3.2)$$

where $(\,)^*$ denotes a free-space Green's function variable and

$$m^2\pi H_1 = \frac{zH(z-1)}{r\sqrt{(z^2\text{-}1)}}, \qquad m^2\pi H_2 = \frac{zH(z-m)}{r\sqrt{(z^2 - m^2)}},$$

$$H_{12} = (z^2 - 1)H_1 + \left(1 - \frac{z^2}{m^2}\right)H_2, \qquad z = \frac{s}{r}. \quad (3.3)$$

4. Problem 2. The governing equations follow from those for the concentrated force problem by replacing (2.3) with $\mathbf{B} = \mathbf{0}$ and (2.4) with the conditions

$$\mathbf{T}^{\pm} = -\mathbf{T}^* \quad (4.1)$$

for $y = \pm 0$, $x > 0$. Figure 1b shows that $r = r(x)$ and $\theta = \theta(x)$ in (4.1), where

$$r(x) = \sqrt{(x^2 + d^2 + 2xd\cos\psi)}, \quad r\sin\theta(x) = d\sin\psi,$$

$$r\cos\theta(x) = x + d\cos\psi. \quad (4.2)$$

The characteristic length d in (4.2) complicates a direct attempt to solve Problem 2 by transform [10] and Wiener-Hopf [11] techniques because the sectionally analytic functions in the transform space will not be related in a standard manner.

To minimize the complication of the characteristic length in the solution of Problem 2, we first consider a related problem, Problem 3, which is identical to Problem 2 except that (4.1) is replaced by

$$\mathbf{T}^{\pm} = \mathbf{N}\delta(x - h)\delta(s - t), \qquad (h, t) > 0, \quad (4.3)$$

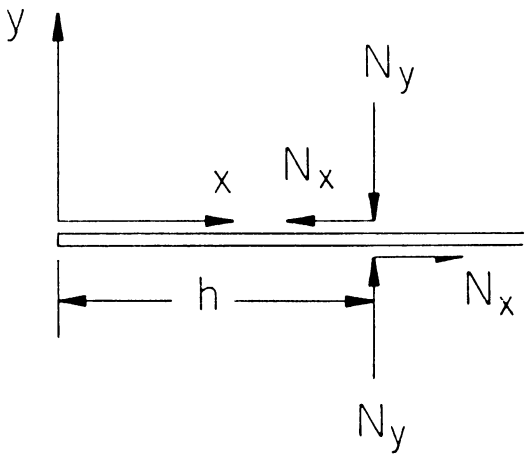

FIG. 2. Geometry for Problem 3.

along $y = \pm 0$, $x > 0$. As seen in Fig. 2, Problem 3 defines a crack with both surfaces subjected to tangential (N_x) and normal (N_y) concentrated forces at a fixed distance h from the crack edge at an instant $t > 0$. Clearly, the solution to Problem 2 can be obtained by substituting $-\mathbf{T}^*$ for $\mathbf{N}$ with (h, t) replacing (x, s) in (3.3) and (4.2) and then integrating the Problem 3 solution over the ht-plane region defined by $h > 0$, $0 < t < s$ and the Heaviside arguments in (3.3). Problem 3 also has a characteristic length, h. Unlike Problem 2, however, it is isolated in the Dirac function argument in (4.3). As will be seen below, this isolation allows Problem 3 to be solved readily by an indirect approach [12, 13] based on superposition.

5. Problem 3 solution approach. Separation of the unbounded plane everywhere along the crack axis $y = 0$ would reduce Problem 3 to a pair of Lamb's problems [14] for concentrated forces applied on the surfaces of half-planes $\pm y > 0$. It follows, then, that Problem 3 can be viewed as the superposition of the two Lamb's problems with the problem of an unbounded cracked plane with no crack surface loading, but a displacement discontinuity extending ahead of the crack edge. The discontinuity is chosen to cancel out the surface displacements generated on the regions $x < 0$ of the two half-planes by the Lamb's problem solutions. This latter problem will be designated as Problem 4. The Lamb's problem-generated surface displacements are presented in Sec. 5.1. Their form suggests the method by which Problem 4 is solved in Sec. 5.2.

5.1. *Surface displacements in Lamb's problem.* Equations (2.1), (2.2) and $\mathbf{B} = \mathbf{0}$, (2.5) and the radiation conditions govern the Lamb's problems when $y \neq 0$ while (4.3) holds for all $y = \pm 0$. Solution of these equations [15] for the surface displacement $\mathbf{u}^-$ for $\pm(h - x) > 0$, $s - t > 0$ in the half-plane $y < 0$ yields

$$(s - t)\mathbf{u}^- = \mathbf{U}^-(q)H(q - 1), \qquad |x - h|q = s - t, \tag{5.1a, b}$$

$$\pi\mu\mathbf{U}^-(q) = N_x \operatorname{Im}\left(-m^2 q \frac{b}{R}, \pm \frac{P}{R} q^2\right) + N_y \operatorname{Im}\left(\pm \frac{P}{R} q^2, m^2 q \frac{a}{R}\right), \tag{5.2}$$

$$P = J - 2ab, \quad J = m^2 - 2q^2, \quad R = 4q^2ab - J^2,$$
$$a = \sqrt{(1-q)^2}, \quad b = \sqrt{(m^2 - q^2)}, \tag{5.3}$$

while $\mathbf{u}^+$ for $y > 0$ follows from (5.2) by reversing the (a, b)-term signs. The function R is the Rayleigh function, and the r.h.s. of (5.2) is evaluated for $\mathrm{Im}(q) = -0$.

5.2. *Problem* 4 *and its solution.* Equations (5.1)–(5.3) indicate that, for a given value of the ratio $|x - h|/(s - t)$ – say c, the corresponding values $\mathbf{U}^{\pm}(1/c)$ in effect radiate from the point $x = h$ with the non-dimensionalized speed c. Since $(s - t)/|x - h| > 1$, the speeds for all $\mathbf{U}^{\pm}$-values on the half-plane surface regions $x < 0$ at a given $s - t > 0$ will lie in the range $h/(s - t) < c < 1$. This suggests that Problem 4 be solved by first considering the cracked half-plane disturbed by a point displacement discontinuity of constant value $\mathbf{e}$ which appears at the crack edge at $s = 0$ and subsequently travels over the crack surface with a constant non-dimensionalized speed c.

The governing equations for this problem when $y \neq 0$ are (2.1), (2.2) with $\mathbf{B} = \mathbf{0}$, (2.5) and the radiation conditions, while for $y = 0$

$$\mathbf{u}^- - \mathbf{u}^+ = \mathbf{e}\delta(x + cs) \quad (x > 0), \qquad \mathbf{T}^{\pm} = \mathbf{0} \quad (x < 0). \tag{5.4a, b}$$

These equations have no characteristic length, and are easily solved by transform/Wiener-Hopf techniques in a standard [12, 13] fashion. It can be shown that any scalar field variable in the solution has the general form $\mathbf{e} \cdot \mathbf{f}(x, y, s, c)$, where $(\cdot)$ denotes the scalar product.

Now, if the discontinuity appears at the crack edge at $s = t + h/c$ instead of $s = 0$ and $\mathbf{e}$ is replaced by $[\mathbf{U}^+(1/c) - \mathbf{U}^-(1/c)]\,dc$, the general form can be integrated w.r.t. c over the range $h/(s - t) < c < 1$ to give the corresponding field variable for Problem 4.

6. Problem 3 solution. The discussion above implies that if F_3 and $F_L^{\pm}$ are corresponding field variables for Problem 3 and the Lamb's problems for $\pm y > 0$, then

$$F_3 = F_L^{\pm} + \int_{h/(s-t)}^{1} [\mathbf{U}^-(1/c) - \mathbf{U}^+(1/c)] \cdot \mathbf{f}(x, y, s - t - h/c, c)\, dc \tag{6.1}$$

for $\pm y \geqslant 0$, where the integration is the Problem 4 contribution. As a demonstration, consider $F_3 = u_x^+ - u_x^-$ along $y = 0$, $x < 0$: From (5.1) and (5.4) we have

$$f_x = \delta[c(s - t) + x - h], \quad f_y = 0, \quad F_L^+ - F_L^- = \frac{1}{s - t}[U_x^+(q) - U_x^-(q)] \tag{6.2a - c}$$

in (6.1). The sifting property of the Dirac function and (5.1) show that the integral in (6.1) yields the negative of (6.2c) and thus $u_x^+ - u_x^-$ appropriately vanishes.

Subsequent interest will focus on the crack edge stress field for the concentrated force problem. It is readily shown that $\mathbf{T}_L$ is not singular near the crack edge but that

$$\mathbf{f} = \frac{\mu(1 - m^2)}{2\pi m^2} \frac{1}{\sqrt{(s)^3}\sqrt{|x|}} \frac{k(b_+, a_+)}{(k + n)G_+(k)}, \qquad k = \frac{1}{c}, \tag{6.3}$$

$$a_{\pm} = \sqrt{(1 \pm k)}, \qquad b_{\pm} = \sqrt{(m \pm k)}, \tag{6.4}$$

$$\ln G_{\pm}(k) = -\frac{1}{\pi} \int_1^m \frac{1}{w \pm k} \tan^{-1}\left(\frac{4w^2|a|b}{J^2}\right) dw \tag{6.5}$$

for $\mathbf{T}$ when $y = 0$, $x \to -0$, where the integrand terms in (6.5) as defined by (5.3) are functions of w. Here $1/n$ is the non-dimensionalized Rayleigh wave speed, where $n > m > 1$ and $R(\pm n) = 0$. Thus, substituting (5.1) and (6.3) into (6.1) yields a formal result for $\mathbf{T}_3$ just ahead of the crack edge. Following [12, 13], the integrations in this result can be simplified by introducing the integration variable $k = 1/c$ and, in some cases, performed explicitly by the Cauchy residue theorem. Then, for $y = 0$, $x \to -0$ (6.1) yields

$$\sqrt{|x|}\mathbf{T}_3 = (N_x K_x, N_y K_y) \tag{6.6}$$

where the x and y-components of the r.h.s. are the Mode II and Mode I dynamic stress intensity factors. For $s - t > nh$ $\mathbf{K} = \mathbf{0}$, while for $h < s - t < mh$

$$\sqrt{(h)}^3\mathbf{K} = \int_1^v \frac{\mathbf{g}(k)}{\sqrt{(v-k)}^3}\,dk,$$
$$\mathbf{g}(k) = \frac{(1-m^2)}{\pi^2 m^2}\frac{(k+n)}{|R|^2} G_+ |a_-| (2k^2 bb_- a_+, -J^2) \tag{6.7}$$

where $hv = s - t$, while for $mh < s - t < nh$

$$\sqrt{(h)}^3\mathbf{K} = \frac{-\mathbf{C}}{\sqrt{(n-v)}^3}, \qquad 4\pi\mathbf{C} = \frac{1}{G_-(n)}(\sqrt{(n-m)}, 2\sqrt{(n-1)}). \tag{6.8}$$

In (6.7) the integrand terms as defined by (5.3), (6.4) and (6.5) are functions of k.

7. Concentrated force problem solution: crack edge stresses. With the Problem 3 solution in hand, the Problem 2 solution follows by integration w.r.t. (h, t) as already indicated in Sec. 4. The concentrated force solution is then obtained by superposing the Problem 1 solution. To illustrate the process involved while showing some solution behavior aspects, we examine $\mathbf{T}$ just ahead ($y = 0$, $x \to -0$) of the crack. The Problem 1 contributions to $\mathbf{T}$ are in general bounded at $(x, y) = 0$ so that only the Problem 2 component is required. To obtain this component, N_x and N_y in (6.6) must be replaced by $-T_x^*$ and $-T_y^*$ with (h, t) playing the role of (x, s) in (3.3) and (4.2), and the result integrated w.r.t. (h, t) as indicated in Sec. 4. From (6.3) and (6.1) the ht-plane integration areas for the H_1 and H_2-contributions are found to have the forms illustrated schematically in Figs. 3a and 3b, respectively. The cross-hatchings (|||) and (///) show the regions where, respectively, (6.7) and (6.8) govern. The actual computation of the h, t and k-integrations is made more efficient as follows:

The fan-shaped ht-regions are more simply described in terms of the polar coordinates (ρ, ω) defined by

$$\rho\cos\omega = s - t, \qquad \rho\sin\omega = h. \tag{7.1}$$

The resulting (ρ, ω)-integrations can then be more efficiently performed and the branch-cut singularities in the H_i-terms extracted analytically by introducing the dimensionless integration variables (X, Ω) and the dimensionless independent variable τ defined by

$$\tan\omega = X, \qquad \rho\cos\omega = r_i d(1 + \sin\Omega),$$
$$\rho\sin\omega = r_i X d(1 + \sin\Omega), \qquad \tau = s/d \tag{7.2}$$

in those terms involving H_i, where

$$2(1 - X^2)r_1 = \tau + X\cos\psi - \sqrt{}\left[(\tau X + \cos\psi)^2 + (1 - X^2)\sin^2\psi\right], \tag{7.3}$$

$$2(1 - m^2X^2)r_2 = \tau + m^2X\cos\psi - m\sqrt{}\left[(\tau X + \cos\psi)^2 + (1 - m^2X^2)\sin^2\psi\right]. \tag{7.4}$$

Finally, the branch-cut singularities arising in (6.7) and (6.8) can be extracted analytically by introducing the variable changes

$$k = 1/c, \qquad 2mX = mc + 1 + (mc - 1)\sin\Omega_x \tag{7.5}$$

in the integrations involving (6.7) and

$$2mX = n + m + (n - m)\sin\omega_x \tag{7.6}$$

in the integrations involving (6.8). It follows that for $y = 0$, $x \to -0$,

$$\sqrt{}|x|\mathbf{T} = \mathbf{K} \tag{7.7}$$

where the mode II and mode I dynamic stress intensity factors K_x and K_y are

$$\sqrt{}dK_\alpha = \int_{1/m}^{1} \frac{g_\alpha(1/c)}{\sqrt{}c} \int \frac{L_\alpha(X) - L_\alpha(c)}{c - X} d\Omega_x\, dc$$

$$+ \frac{C_\alpha}{\sqrt{}(n)^3} \int \frac{L_\alpha(X) - L_\alpha(1/n)}{1/n - X} d\omega_x. \tag{7.8}$$

Here $\alpha \equiv x$ or y, $\mathbf{g}$ and $\mathbf{C}$ are defined in (6.7) and (6.8). The vector $\mathbf{L}$ is given by

$$\frac{\pi\mathbf{L}(X)}{\sqrt{}|X + 1/m|} = \sum \int \left[\frac{\mathbf{P}_i(\theta_i)}{D_i} + \frac{r_i D_i}{R_i^2}\mathbf{Q}_i(\theta_i)(1 - \sin\Omega)\right]\left[\tau - r_i(1 + \sin\Omega)\right]\frac{d\Omega}{R_i} \tag{7.9}$$

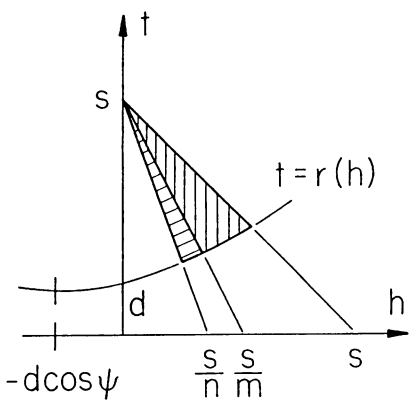

FIG. 3a. Integration regions in ht-plane for H_1-contributions.

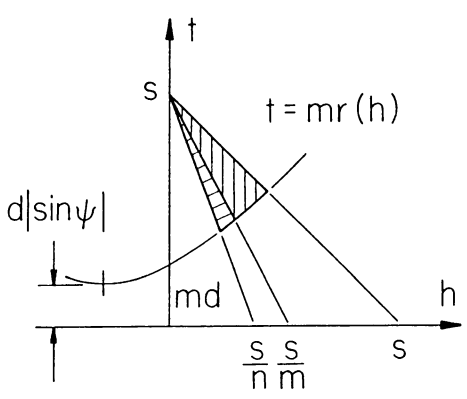

FIG. 3b. Integration regions in ht-plane for H_2-contributions.

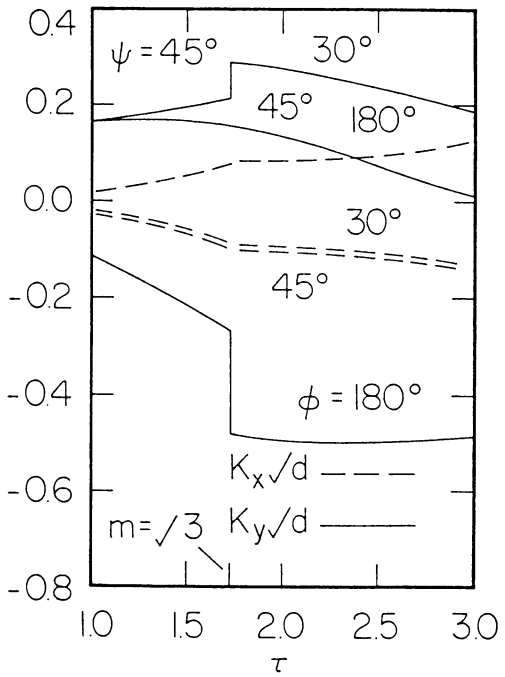

FIG. 4. Dynamic stress intensity factors for $\psi = 45°$.

where summation w.r.t. the index i is over the range (1, 2) and

$$D_1 = \sqrt{\left[2\left(\frac{\tau + X\cos\psi}{1 - X^2}\right) + (\sin\Omega - 3)r_1\right]}\sqrt{(1 - X^2)}, \tag{7.10}$$

$$D_2 = \sqrt{\left[2\left(\frac{\tau + m^2X\cos\psi}{1 - m^2X^2}\right) + (\sin\Omega - 3)r_2\right]}\sqrt{|1 - m^2X^2|}, \tag{7.11}$$

$$R_i = \sqrt{\left[1 + r_i^2X^2(1 + \sin\Omega)^2 + 2r_iX(1 + \sin\Omega)\cos\psi\right]}. \tag{7.12}$$

In (7.9) $\mathbf{P}_1$ and $\mathbf{Q}_1$ follow from (3.1) and (3.2) as

$$2m^2\mathbf{P}_1(\theta) = \cos(\phi - \theta)(\sin 2\theta, m^2 - \cos^2\theta), \tag{7.13}$$

$$m^2\mathbf{Q}_1(\theta) = -(\sin(\phi - 3\theta), \cos(\phi - 3\theta)). \tag{7.14}$$

for $\tau > 1$ and vanish otherwise. Similarly,

$$2\mathbf{P}_2(\theta) = \sin(\phi - \theta)(\cos 2\theta, -\sin 2\theta), \qquad \mathbf{Q}_2(\theta) = -\mathbf{Q}_1(\theta) \tag{7.15}$$

for $\tau > m$ but vanish otherwise. In (7.13)–(7.15), θ_i follows from (5.1) and (7.2) as

$$R_i\sin\theta_i = \sin\psi, \qquad R_i\cos\theta_i = r_iX(1 + \sin\Omega) + \cos\psi. \tag{7.16}$$

In (7.8) and (7.9), the symbol $\int$ denotes integration over the range $(-\pi/2, \pi/2)$.

Equation (7.8) is plotted vs. $\tau \geqslant 1$ in Fig. 4 for the typical value $m = \sqrt{3}$, $\psi = 45°$ and various values of ϕ. These curves indicate that the Mode I intensity factor generally dominates the crack edge stress field.

8. Discussion. The results presented here show that exact expressions for the 2D dynamic solution of a concentrated force near a semi-infinite crack in an unbounded plane can be derived, even though a characteristic length is involved, by breaking the

problem into a series of simpler problems. The resulting solution expressions for the crack edge stress field are in the form of multiple singular integrations. However, by integration variable changes, the singularities can be extracted analytically and the integrations themselves kept in simple forms. For example, the formidable-appearing Ω-integrations in (7.9) are essentially of the simple type

$$\int \left(\frac{1 + a_1 \sin \Omega}{1 + a_3 \sin \Omega + a_4 \sin^2 \Omega} \right) \sqrt{\left(\frac{1 + a_3 \sin \Omega + a_4 \sin^2 \Omega}{1 + a_2 \sin \Omega} \right)^{\pm 1}} \, d\Omega. \tag{8.1}$$

Here the a_i are independent of Ω, so that the integrations are easily computed by standard Gaussian quadrature.

Modern computational methods and equipment do not necessarily require such effort in integration preparation. However, the present results were derived with the idea that the solution expressions might be used in the solution of transient wave-scattering problems. Thus, they should add little to the computational and numerical precison burden, while allowing analytical manipulation. This latter property is manifested in (7.8), for example: the Problem 1 components (3.1) and (3.2) and the Problem 3 components are readily discerned in the **g**, **C** and **L**-terms.

In summary, then, the results given here show how the dynamic 2D problem of a concentrated force near a semi-infinite crack in an unbounded solid can be solved exactly and in a convenient form, even though a characteristic length is involved. The solution itself can then be used to generate transient solution representations for problems involving in-plane loading and a stationary, external, traction-free crack. The crack, and its attendant singularities, are automatically built into the representation.

As indicated above and in section 1, such representations are useful in wave-scattering studies, where complicated incident wave forms and possibly irregular material boundaries already provide formidable solution difficulties. However, an even more immediate application is currently in preparation: Inelastic zones near crack edges can be modeled as dislocation arrays [16], so that the study of non-purely brittle fracture becomes one of crack-dislocation interaction.

In [17], the problem of screw dislocation motion near a Mode III crack was solved directly. The more difficult problem of edge dislocation motion near a Mode I–II crack presently defies a direct approach. However, by combining the Burridge-Knopoff [6] body force equivalents for dislocations with the results presented here, the problem solution—in particular, the crack edge stress field—can be readily calculated. The most difficult mathematical operation involves a convolution w.r.t. time.

REFERENCES

[1] J. D. Achenbach, Y. H. Pao and H. F. Tiersten, *Application of elastic waves in electrical devices, non-destructive testing and seismology*, Northwestern University, Evanston, 1976.

[2] V. K. Varadan and V. V. Varadan, *Acoustic, electro magnetic and elastic wave scattering—Focus on the T-matrix approach*, Pergamon, Oxford, 1980.

[3] I. Stakgold, *Green's functions and boundary value problems*, Wiley, New York, 1979.

[4] J. T. Fokkema and P. M. vandenBerg, *Elastodynamic diffraction by a periodic rough surface (stress-free boundary)*, Journal of the Acoustics Society of America **62**, 1095–1101 (1977)

[5] T. Mura, *Micromechanics of defects in solids*, Nijhoff, The Hague, 1982.
[6] R. Burridge and L. Knopoff, *Body force equivalents for seismic dislocations*, Bulletin of the Seismological Society of America **54**, 1875–1888 (1964)
[7] J. D. Achenbach, *Wave propagation in elastic solids*, North-Holland, Amsterdam, 1973.
[8] G. F. Carrier and C. E. Pearson, *Partial differential equations*, Academic, New York, 1976
[9] L. M. Brock, *Non-uniform edge dislocation motion along an arbitrary path*, Journal of the Mechanics and Physics of Solids **31**, 123–132 (1983)
[10] I. N. Sneddon, *The use of integral transforms*, McGraw-Hill, New York, 1972.
[11] G. F. Carrier, M. Krook and C. E. Pearson, *Functions of a complex variable*, McGraw-Hill, New York, 1966
[12] L. B. Freund, *The stress intensity factor due to normal impact loading of the faces of a crack*, International Journal of Engineering Science **12**, 179–190 (1974)
[13] L. M. Brock, *Shear and normal impact loadings on one face of a narrow slit*, International Journal of Solids and Structures **18**, 467—477 (1982)
[14] H. Lamb, *On the propagation of tremors over the surface of an elastic solid*, Philosophical Transactions of the Royal Society of London **A203**, 1–42 (1904)
[15] L. M. Brock, *The effects of displacement discontinuity derivatives on wave propagation-III. body and point forces in elastic half-spaces*, International Journal of Engineering Science **19**, 949–957 (1981)
[16] B. A. Bilby and J. D. Eshelby, *Dislocations and the theory of fracture*, in: Fracture, Vol. 1, H. Liebowitz, ed., Academic, New York, 1968..
[17] L. M. Brock, *The dynamic stress intensity factor due to arbitrary screw dislocation motion*, Journal of Applied Mechanics **50**, 383–389 (1983)